

Effects of low-dose sodium nitrite on the structure of yak meat myoglobin during wet curing

Guoyuan Ma^{*}, Zhuo Wang, Qunli Yu, Ling Han, Cheng Chen, Zhaobin Guo

College of Food Science and Engineering, Gansu Agricultural University, 1#, Yingmen Village, Anning, Lanzhou, Gansu 730070, China

ARTICLE INFO

Keywords:

Yak meat
Myoglobin
Nitrosylation
FTIR
Laser Micro-Raman spectroscopy
LC-ESI-MS/MS

ABSTRACT

The effects of low doses of sodium nitrite on yak meat colouring, myoglobin oxygenation status, myoglobin aggregation and myoglobin structure were evaluated using Fourier transform infrared spectroscopy, laser micro-Raman spectroscopy and liquid chromatography-electrospray ionization tandem mass spectrometry. The results showed that the yak meat redness value increased steadily relative to that of the control after the addition of low dose sodium nitrite. The nitrosomyoglobin level gradually increased and was significantly higher in the sodium nitrite-treated group than in the control group. The secondary structures were also transformed. The C_α-N bond extended and then contracted, the area of the haem core decreased and then increased and the frequency of contraction increased. A total of 34 nitrosylated peptides were identified, of which 15 were stable and 19 were unstable. These findings show that low doses of sodium nitrite facilitated the dynamic transformation of the myoglobin nitrosylated peptide fragment, which in turn preserved the colour of the meat.

Introduction

The colour and quality of meat products may have a significant effect on consumer decisions when purchasing meat products; therefore, colour is a very significant factor when choosing meat products (Ram-anathan et al., 2020). Myoglobin is the main colouring substance in meat products (Suman & Joseph, 2013). Yaks are mainly found in China on the Tibetan Plateau and have a high myoglobin content (Chen et al., 2015), which means their meat is dark reddish-brown in colour. Therefore, sodium nitrite is often added during processing to give yak meat a vivid red colour.

Nitrite can be broken down to NO, which reacts with myoglobin (Mb) in meat to form a red nitroso compound (Skibsted, 2011; Vossen & Smet, 2015), which is more stable. Nitrites are usually added to meat and meat products during the curing process to stabilize the meat colour (Bozkurt & Erkmen, 2004). The antioxidant capacity of western ham is positively correlated with the amount of sodium nitrite added and varies with storage time when the amount of sodium nitrite added is altered (Feng et al., 2016). During thermal processing, sodium nitrite reacts with other compounds in meat to form nitroso compounds, which have antioxidant properties (Denisa et al., 2018; Sasykova et al., 2019). Sodium nitrite reacts with the carbon-carbon double bonds in unsaturated fatty acids and inhibits oxygen radical attacks on lipids, which

means that it also has anti-lipid oxidation properties (Haile et al., 2013). Although the role of sodium nitrite in meat products has been studied, there have been no reports on the colour protection mechanisms associated with sodium nitrite, particularly how it affects myoglobin structure and the nitrosylation binding site.

Raman spectroscopy has made great progress as an important research method for the molecular or complex molecular system. It has been applied in investigations in many fields (Das & Agrawal, 2011). Protein Raman spectroscopy not only reflects the skeletal vibration of the peptide chain but also reflects changes in the microenvironment around the side chains. Its advantage lies on its wide application ranges. Protein Raman spectroscopy can be used both in non-aqueous and aqueous solutions, such as powders and especially, colloids (Eberhardt et al., 2015). The Fourier transform infrared spectroscopy (FTIR) method can be customized not only for qualitative analysis of the protein secondary structures but also for quantitative analysis. Fourier deconvolution and second derivative can be used to further decompose the peaks that cannot be resolved by the amide band in the infrared spectrum into multiple subpeaks. Fourier deconvolution and second derivative can also indicate the peak positions of the subpeaks and fit the curve of the quantitative analysis of the protein secondary structure content (Zheng et al., 2017). Novel detection technologies, including omics technology (Kuang et al., 2012), nanotechnology (Wang et al.,

^{*} Corresponding author.

E-mail address: 297493468@qq.com (G. Ma).

2020), etc., are increasingly prominent in the detection of biological macromolecules. However, the use of FTIR spectroscopy and laser micro-Raman spectroscopy to study the role of NaNO_2 in the structure of myoglobin has not been reported.

Therefore, this study assessed yak meat colouration, myoglobin oxidation state, dityrosine content, turbidity changes, secondary structure, interatomic (molecular) interactions and nitrosylated peptides and sites during wet curing using Fourier transform infrared (FTIR) spectroscopy, laser micro-Raman spectroscopy and liquid chromatography-tandem mass spectrometry techniques (LC-ESI-MS/MS). We also discuss the key role of sodium nitrite in this process and finally provide a potential mechanism for meat colour stabilization by sodium nitrite.

Materials and methods

Sample collection and processing

Five male yaks (mean age: 2–3 yr, mean live weight: 200 ± 10 kg) were randomly obtained from the same pastureland in the Tibetan Autonomous Prefecture of Gannan, Gansu Province, China, on an equal diet from the same batch of feed. Samples (5 kg) of *longissimus dorsi* muscles (from the 12th thoracic vertebra to the 5th lumbar vertebra) were collected directly after humane slaughter at commercial yak meat processing companies (Gannan Minsheng Tibetan Yak Breeding Farmers Cooperative, Hezuo City, Gansu province, China) according to the 'Operating Procedures of Cattle Slaughter' - the National criterion P.R. of China (China, 2018). Visible fat and connective tissue were removed, and samples were sliced into cubes of $10 \times 5 \times 3$ cm³ and then divided into two sections. The 90 mg/L sodium nitrite solution (Ma et al., 2019) was injected into the treatment group. Each sample cube was injected by needle injection at distance of 1.5 cm, with a needle penetration depth of 1.5 cm (approximately half the thickness of the meat). After removal of the needle, each injection site was subjected to a gentle massage for 20 s to ensure the uniform diffusion of NaNO_2 in the meat. To achieve a weight of 120 % of the original meat weight reported, the treatment group was injected to ensure that the amount of NaNO_2 solution was equal to 20 % of the initial meat weight; this was not achieved in the control group. Both samples were processed for storing at 4 ± 0.5 °C and taken from the refrigerator for calculation and examination at the end of days 0 (no injection), 1, 3, 5, and 7. The experiment was repeated three times.

Determination of redness values (a^*)

The values of muscle redness (a^*) were calculated by a colourimeter (CR410) (Claus & Du, 2014). At each point in time, three samples were obtained from each of the two groups. Fresh cuts were measured for 20–30 min after air exposure.

Extraction of myoglobin

By reference to the Thiansilakul et al. (2012) process, myoglobin was extracted. Muscle samples were mixed at a stock-to-solution ratio of 1:3 with an extraction buffer solution (10 mM Tris-HCl, pH 8.0, containing 1 mM EDTA and 10 g/L Triton X-100, 0–4 °C). At 10,000 rpm for 1 min, the supernatant was then homogenized, centrifuged at 10,000 rpm for 10 min at 4 °C and filtered onto filter paper. Impurity proteins were removed using 50 % and 90 % saturated ammonium sulphate, respectively, and the precipitate was solubilised with a minimum volume of 5 mM Tris-HCl pH 8.5 pre-cooled (4 °C) buffer solution, followed by dialysis using 5 mM Tris-HCl pH 8.5 for 24 h. The dialysate was purified using a Sephadex G-100 column (1.5×100 cm). The mobile phase was 5 mM Tris-HCl pH 8.5 buffer. The UV absorbance values were monitored at 280 nm and the eluate was collected using an automatic collector. The concentration of myoglobin in the eluate was determined using the Biuret method.

Determination of myoglobin oxidation status

The content of myoglobin was set to 1 mg/mL. Simultaneous UV spectrophotometry reported the absorbance values at 525, 545, 565 and 572 nm and the relative contents of oxymyoglobin (OMb) and met-myoglobin (MMb) were determined according to the Tang et al. (2004).

Determination of myoglobin dityrosine content

The content of myoglobin was set to 2 mg/mL. Fluorophotometry (Morzel et al., 2006) calculated the dityrosine content at an emission wavelength of 420 nm (slit 5 nm) and an excitation wavelength of 325 nm (slit 5 nm). Relative fluorescence values were expressed as the dityrosine content (Arbitrary Units (AU)).

Determination of turbidity of myoglobin

The turbidity was measured by UV spectrophotometry and the absorbance values at 340 nm were recorded and expressed as OD values (Kaspchak et al., 2019).

Measurement of secondary structure changes in myoglobin

Measurements were made at $400\text{--}4000$ cm⁻¹ using a scanning FTIR. Subsequently, the Peakfit 4.12 package for Gaussian fitting study of myoglobin secondary structure shifts was used to derive data from 1600 to 1700 cm⁻¹ (Li et al., 2019).

Myoglobin Raman spectroscopy determination

With slight modifications by Farhane et al. (2016), laser micro-Raman spectroscopy was identified. As a laser micro-Raman spectrometer, the Lab Ram HR800 was used. The parameters were set as follows: 532 nm laser wavelength, 7.63 mW power, 200 μm slit diameter, 400 level/cm grafting density, 200–1800 cm⁻¹ scan range and 20 s scan time. Furthermore, three integrations of phenylalanine as the normalization factor were performed. The curves were smoothed after collecting the raw spectra using Origin 8.0 software to exclude other interferences and the peaks were fitted to measure the peak areas in the 1335–1650 cm⁻¹ range.

Determination of nitrosomyoglobin content

The reaction solution was 80 % acetone and 20 % water. The material to liquid ratio was 1:5, homogenised and centrifuged at 5000g for 5 min. The supernatant was scanned for spectra from 500 to 700 nm, and the absorbance was measured at 640 nm multiplied by 680 to give the total heme content (ppm), and at 540 nm multiplied by 290 to give the nitrosomyoglobin content (ppm) (Wójciak & Dolatowski, 2015).

Visible spectroscopy of myoglobin

Compared to Honikel (2008), a 50 mL polypropylene centrifuge tube was transferred to the muscle (1 g), then 10 mL cold 5 mM Tris-HCl (pH 8.5) was applied. The mixture was homogenized at 13,000 rpm for 20 s and then centrifuged at 4 °C at 3,000 g for 30 min. The supernatant was filtered onto filter paper. In the 510 to 610 nm scale, the myoglobin solution and nitrosomyoglobin (NOMb) absorption spectrums were measured.

Myoglobin nitrosylation assay

Sample preparation

All samples in the lysis buffer was homogenized (4 % SDS, 1 mM DTT, 150 mM Tris-HCl pH 8.0). The homogenate was incubated in boiling water for 3 min and then placed in an ice bath. The crude extract

was clarified at 16000 g and 25 °C for 10 min and BCA protein assay reagent was used to assess protein content (Bio-Rad, Hercules, CA, USA). The supernatants were then stored at -80 °C until needed.

Protein digestion

Digestion of protein (250 µg for each sample) was performed according to the FASP procedure described by (Luber et al., 2010; Schwanhäusser et al., 2011). Briefly, detergents, DTT, and other low-molecular-weight components were removed using 200 µL UA buffer (8 M urea, 150 mM Tris-HCl, pH 8.0) by repeated ultrafiltration (Microcon units, 10 kDa) combined with centrifugation. Then, 100 µL of 0.05 M iodoacetamide in UA buffer was added to block reduced cysteine residues and the samples were incubated for 20 min in the dark. The filter was washed three times with 100 µL UA buffer and then twice with 100 µL 25 mM NH₄HCO₃. Finally, the protein suspension was digested overnight with 3 µg trypsin (Promega, Madison, WI, USA) in 40 µL 25 mM NH₄HCO₃ at 37 °C and the resulting peptides were collected as a filtrate.

Liquid chromatography (LC)-Electrospray ionization (ESI) tandem MS (MS/MS) analysis by Q Exactive

The peptide of each sample was desalted on C18 Cartridges (Empore™ SPE Cartridges C18 (standard density), bed I.D. 7 mm, volume 3 mL, Sigma), then concentrated by vacuum centrifugation and reconstituted in 40 µL of 0.1 % (v/v) trifluoroacetic acid. MS experiments were performed on a Q Exactive mass spectrometer that was coupled to Easy nLC (Proxeon Biosystems, now Thermo Fisher Scientific). 5 µg peptide was loaded onto the C18-reversed phase column (Thermo Scientific Easy Column, 10 cm long, 75 µm inner diameter, 3 µm resin) in buffer A (2 % acetonitrile and 0.1 % Formic acid) and separated with a linear gradient of buffer B (80 % acetonitrile and 0.1 % Formic acid) at a flow rate of 250 nL/min controlled by IntelliFlow technology over 60 min. MS data were acquired using a data-dependent top10 method dynamically choosing the most abundant precursor ions from the survey scan (300–1800 *m/z*) for HCD fragmentation. Determination of the target value is based on predictive Automatic Gain Control (pAGC). Dynamic exclusion duration was 25 s. Survey scans were acquired at a resolution of 70,000 at *m/z* 200 and resolution for HCD spectra was set to 17,500 at *m/z* 200. The normalized collision energy was 30 eV and the underfill ratio, which specifies the minimum percentage of the target value likely to be reached at maximum fill time, was defined as 0.1 %. The instrument was run with peptide recognition mode enabled. MS experiments were performed triply for each sample.

Sequence database searching and data analysis

The MS data were analyzed using MaxQuant software version 1.3.0.5. MS data were searched against the UniProtKB bos taurus database (46718 total entries, downloaded 202001010). An initial search was set at a precursor mass window of 6 ppm. The search followed an enzymatic cleavage rule of Trypsin/P and allowed maximal two missed cleavage sites and a mass tolerance of 20 ppm for fragment ions. Carbamidomethylation of cysteines was defined as a fixed modification, while methionine oxidation and all amino acid NO₂ were defined as variable modifications for database searching. The cutoff of global false discovery rate (FDR) for peptide and protein identification was set to 0.01.

Statistical analysis

Using one-way ANOVA by SPSS 20.0.0 (IBM, Armonk, NY, USA), statistical analysis of the discrepancy was done. With Duncan's multiple range checks, significance was calculated among the groups. The level of importance was set at *P* < 0.05.

Results

Changes in meat colour of yak meat

The use of sodium nitrite marinade resulted in the brighter red meat colour of yak meat, as can be seen from Fig. 1a. Compared to the control group *a**, it was 1.60, 5.12, 2.91 and 2.02 higher on days 1, 3, 5 and 7, respectively, with significant differences on days 1, 3 and 5 (*P* < 0.05).

Changes in myoglobin oxidation status

As can be seen from Fig. 1b, the oxymyoglobin (OMb) content of the control group gradually decreased (*P* < 0.05) as the marination time increased. However, on the first day of marination, the OMb content of the sodium nitrite group substantially decreased by 41.20 % (*P* < 0.01). The sodium nitrite group had a significantly lower OMb content than the control group (*P* < 0.01). In the control group, the MMb content increased gradually (*P* < 0.05), whereas in the sodium nitrite-treated group, the MMb content increased and then levelled off (*P* < 0.05) (Fig. 1c).

Myoglobin aggregation

Tyrosine is a sensitive amino acid that is prone to attack by reactive oxygen radicals and its oxidation results in the formation of dityrosine. Fig. 1 shows that the content and turbidity of yak meat myoglobin dityrosine had similar patterns and that they increased over time (*P* < 0.05). The yak meat myoglobin dityrosine content and turbidity in the group with sodium nitrite curing were slightly higher than those in the control group (*P* < 0.01), with values of 3.19, 2.42, 3.44, 1.61 (Fig. 1d), and 0.03, 0.04, 0.04, and 0.02 (Fig. 1e), respectively, at 1, 3, 5, and 7 d, respectively. Thus, sodium nitrite improved the dityrosine content and turbidity of yak meat myoglobin during wet curing.

Structural changes in myoglobin

Changes in the secondary structure content of yak meat myoglobin

Fig. 2a shows that as time progressed, the α-helix content of the control group first increased and then decreased, the β-sheet content decreased, the β-turn content first decreased and then increased and the random coil content first increased and then decreased. In the sodium nitrite treatment, the α-helix content increased and then decreased, the β-sheet content increased and then decreased, the β-turn content decreased and then increased and the random coil content increased and then decreased. The α-helix content was 0.99 % lower, the β-sheet content was 4.48 % higher, the β-turn content was 4.71 % lower and the random coil content was 0.58 % higher on the third day in the sodium nitrite-treated group compared to those in the control group. Furthermore, the α-helix content was 2.02 % lower, the β-sheet content was 0.28 % higher, the β-turns content was 0.08 % lower and the random coil content was 1.27 % higher on the seventh day in the sodium nitrite-treated group compared to those in the control group.

Laser micro-Raman spectroscopy detection qualitative analysis

Fig. 2b is the original Laser micro-Raman spectroscopy spectrum. The findings in Table 1 and Table 2 were obtained after examining the initial spectrum of Laser micro-Raman spectroscopy, according to the band's data from Ma et al. (2019).

Heme ring skeleton vibration correlation band. The control group demonstrated a stretching pattern with increases in C_α-N bond length, C_α-N symmetrical stretching (amide I), as seen in Tables 1 and 2. The sodium nitrite-treated group first extended and then contracted, and the C_α-N bond length increased. The peak area for amide II (C_α-C_m symmetrical stretching) decreased and then increased in the control group,

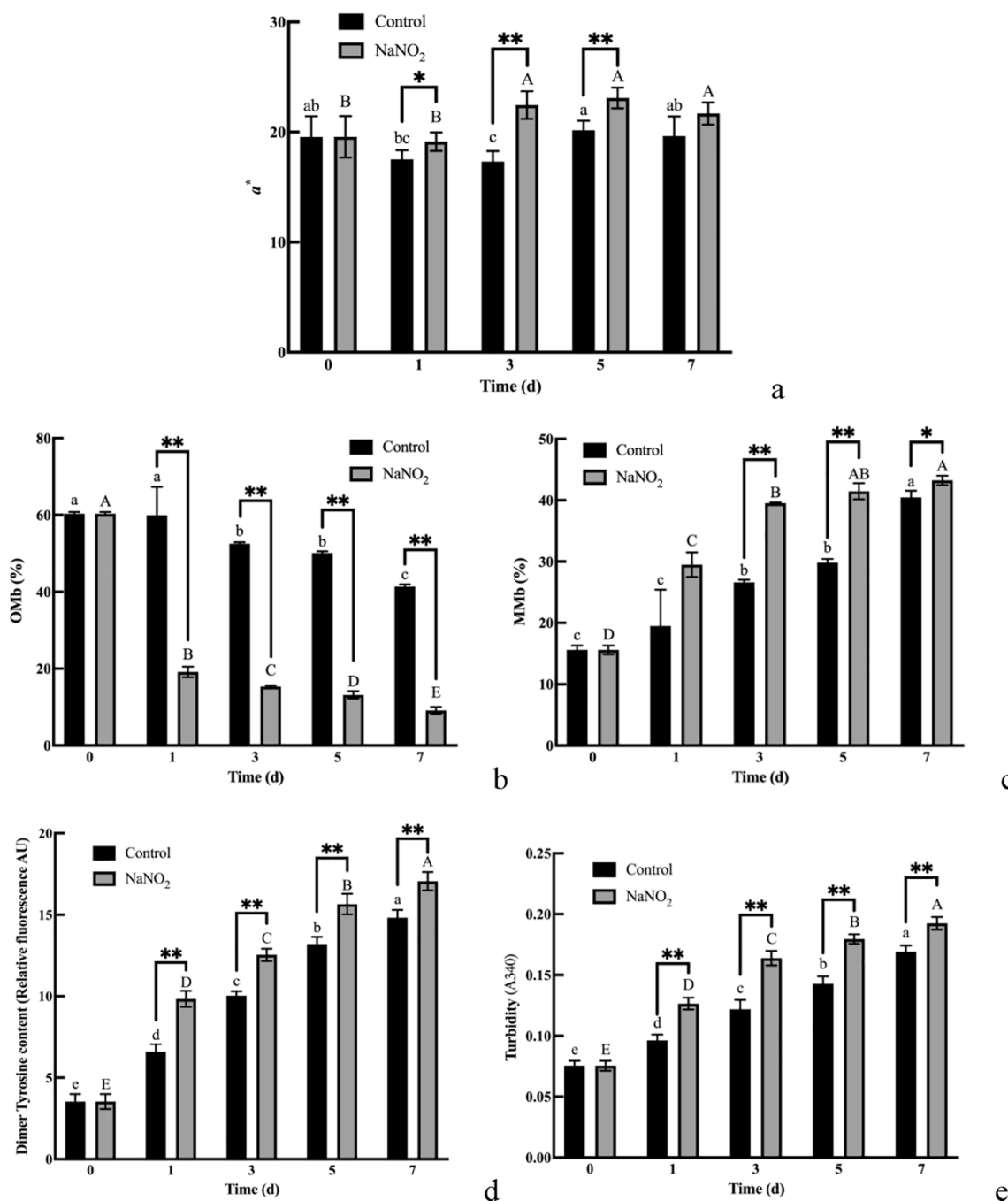


Fig. 1. Effect of sodium nitrite on meat colour, myoglobin oxygenation status and myoglobin aggregation in yak meat. (a) Changes in redness values. (b) Omb content. (c) Mmb content. (d) Dimeric tyrosine content. (e) Changes in turbidity. The small letters indicated the significant difference of the control group and the capital letters indicated the significant difference of the treatment group ($P < 0.05$). The * indicates the significant difference between groups, *: ($P < 0.05$); **: ($P < 0.01$).

and the distance between α -carbon atoms and other carbon atoms increased, suggesting a stretching pattern, but there was no significant difference between the third and seventh days. However, the peak area of the sodium nitrite-treated group decreased and then increased, and the distance between the α -carbon atoms and other carbon atoms first increased and then decreased. In the control and sodium nitrite-treated groups, the peak areas for amide IV and V (C_{α} - C_{β} symmetrical stretching) decreased and then increased, but the length of the amide V C_{α} - C_{β} bond increased and then decreased as time progressed. The control group amide VI (C_{β} - C_{β} Symmetrical Stretching), C_{β} - C_{β} followed a stretching pattern as time progressed, with an increase in bond length and a decrease in peak area. In contrast, C_{β} - C_{β} in the sodium nitrite-treated

group showed a stretching trend with an increase in bond length and a decrease in peak area. There was also an increase in peak area. The amide III (Heme core size) and the control and sodium nitrite group areas tended to decrease and then increase as time progressed. Furthermore, the peak area for the sodium nitrite-treated group on the seventh day was greater than that at 0 h; the bond-to-bond pattern of the control group was extended and the length of the bond increased.

Fe-ligand correlation bands. The bond lengths between the Fe atoms and other atoms in the control group increased over time, indicating a pull-up pattern, as shown in Tables 1 and 2, but the bond lengths between the Fe atoms and the nitrogen and oxygen atoms showed a contraction trend

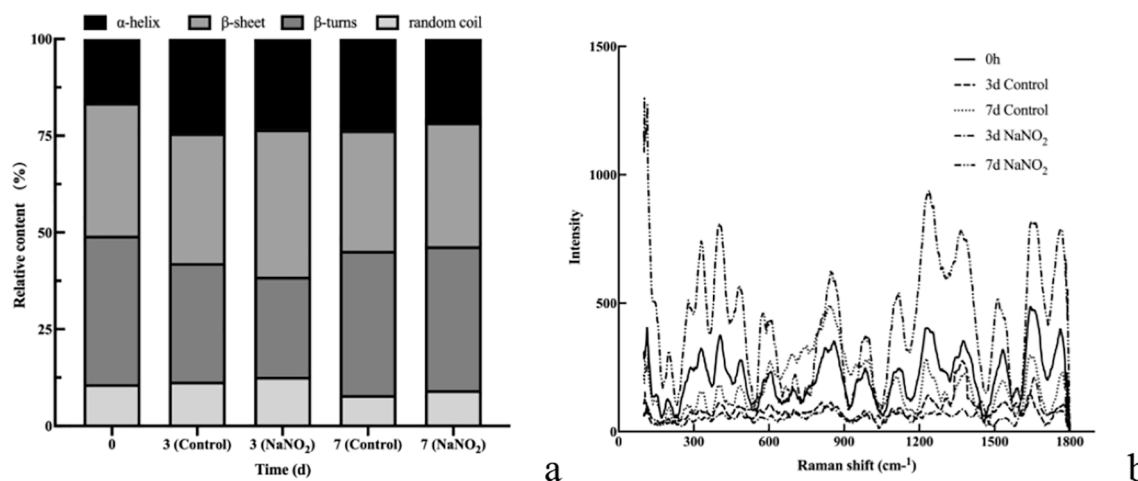


Fig. 2. Effect of sodium nitrite on the structure of myoglobin in yak meat. (a) Changes in secondary structure of myoglobin. (b) Changes in Raman spectra of myoglobin.

Table 1

Peak area (or intensity) of Laser micro-Raman spectroscopy.

Peak Position (cm ⁻¹)	Peak area (or intensity)						
	Control			NaNO ₂			
	0d	3d	7d	0d	3d	7d	7d
1560–1600	5818.82	3702.98	3786.90	5818.82	1326.66	3652.99	
1605–1645	11998.95	3959.26	7333.76	11998.95	3839.41	18184.71	
1550–1590	6288.60	3658.13	4355.44	6288.60	1268.21	5715.99	
1535–1575	8087.26	3745.96	5596.30	8087.26	1653.23	10905.63	
1470–1505	4768.05	2267.80	2410.05	4768.05	952.52	10066.18	
1340–1390	15752.90	12516.30	9967.99	15752.90	3871.26	37006.69	
574	177.59	75.69	144.42	177.59	54.92	454.18	
567	137.28	83.64	146.47	137.28	55.77	424.83	
549	78.91	62.86	114.32	78.91	41.81	125.13	
500	232.88	89.19	150.88	232.88	56.22	456.36	
453	186.99	70.35	98.13	186.99	54.78	432.03	
419	295.53	98.08	132.07	295.53	67.80	691.26	
413	344.09	102.32	158.59	344.09	73.04	758.27	
412	351.13	103.52	164.56	351.13	72.39	769.88	
200–225	2066.52	871.92	1420.04	2066.52	851.14	5415.88	

1560–1600, 1605–1645, 1550–1590, 1535–1575, 1470–1505, 1340–1390 and 200–225 cm⁻¹ are represented by peak areas; 574, 567, 549, 500, 453, 419, 413 and 412 cm⁻¹ are represented by peak intensity.

on the seventh day, which reduced their lengths. The bond lengths increased between the Fe atoms and other atoms in the sodium nitrite-treated group on the third day, indicating a pull-up pattern; however, the bond lengths shortened on the seventh day, which suggested contraction or bending. The peak strength of both groups declined and then increased. There was a decline on the third day in the sodium nitrite-treated group, but the increase on the seventh day was higher than that in the control group.

Fe-His correlation bands. As can be shown from Tables 1 and 2, the bond lengths in the control group between the Fe atoms and the proximal histidine increased over time, indicating a stretching pattern; the bond lengths in the sodium nitrite treated group between the Fe atoms and the proximal histidine first increased and then decreased, showing a stretching and then bending trend. In both cases, the peak area reduced and then increased, with a higher increase in the group treated with sodium nitrite than in the control group on day 7.

Analysis of NOMb content and nitrosation

In the sodium nitrite treated group, the NOMb content of yak meat rose steadily over time ($P < 0.05$) and was slightly higher than in the

control group ($P < 0.01$). The absorbance increased first and then decreased at each wavelength of the sodium nitrite treated group (Fig. 3a, 3b).

The main mass spectra for nitrosated myoglobin were shown in Fig. 3c, 3d, 3e, 3f and 3g. The control and treated groups contained 34 nitrosated peptides, 136 potential nitrosation sites and 17 computer simulation sites. Of these, 44 nitrosylation sites were common to the control and sodium nitrite-treated groups, 14 were unique to the control group, and 6 were unique to the sodium nitrite-treated group. A total of 28 nitrosylation sites were found in the 0 d samples, four of which were obtained through computer simulations. Compared to 0 d, 29 nitrosylation sites were identified in the 3 d control community. There were five new sites, three had disappeared and two were computer simulation sites. A total of 30 sites were detected at 7 d. There were four new sites, two had disappeared and four were computer simulation sites. A total of 24 sites were detected in the 3 d sodium nitrite treatment group, with three new, seven disappeared, and two computer simulation sites, and 26 sites were detected in the 7 d sodium nitrite treatment group, with three new, seven reduced, and two computer simulation sites. The differences between the two groups were shown in Table 3.

Table 2
Qualitative Analysis of Variations of Laser micro-Raman spectroscopy.

Band	Contribution	Control			NaNO ₂		
		0d	3d	7d	0d	3d	7d
VI	Cβ-Cβ Symmetrical stretching	/	Significant Stretch, bond length growth	Significant Stretch, bond length growth	/	Extremely significant Stretch, bond length growth	Stretch, bond length growth
V	Cα-Cβ Symmetrical stretching	/	Extremely significant Stretch, bond length growth	Significant Stretch, bond length growth	/	Extremely significant Stretch, bond length growth	Extremely significant shrinkage, bond length shortening
IV	Cα-Cβ Symmetrical stretching	/	Extremely significant Stretch, bond length growth	Significant Stretch, bond length growth	/	Extremely significant Stretch, bond length growth	Significant Stretch, bond length growth
III	Heme core size	/	Extremely significant Stretch, bond length growth	Significant Stretch, bond length growth	/	Extremely significant Stretch, bond length growth	Significant shrinkage, bond length shortening
II	Cα-Cm Symmetrical stretching	/	Extremely significant Stretch, bond length growth	Extremely significant Stretch, bond length growth	/	Extremely significant Stretch, bond length growth	Extremely significant shrinkage, bond length shortening
I	Cα-N Symmetrical stretching	/	Significant Stretch, bond length growth	Extremely significant Stretch, bond length growth	/	Extremely significant Stretch, bond length growth	Extremely significant shrinkage, bond length shortening
	Fe(II)-C—O Bending vibration	/	Extremely significant Stretch, bond length growth	Significant Stretch, bond length growth	/	Extremely significant Stretch, bond length growth	Extremely Significant bending, bond length shortening
	Fe-O2 Stretching vibration	/	Extremely significant Stretch, bond length growth	Significant Stretch, bond length growth	/	Extremely significant Stretch, bond length growth	Extremely significant shrinkage, bond length shortening
	Fe-NO Stretching vibration	/	Significant Stretch, bond length growth	Significant shrinkage, bond length shortening	/	Significant Stretch, bond length growth	Significant shrinkage, bond length shortening
	Fe(II)—CO Stretching	/	Extremely significant Stretch, bond length growth	Significant Stretch, bond length growth	/	Extremely significant Stretch, bond length growth	Extremely significant shrinkage, bond length shortening
	Fe(III)—CN Stretching	/	Extremely significant Stretch, bond length growth	Extremely significant Stretch, bond length growth	/	Extremely significant Stretch, bond length growth	Extremely significant shrinkage, bond length shortening
	Fe—O—O Bending vibration	/	Extremely significant Stretch, bond length growth	Significant Stretch, bond length growth	/	Extremely significant Stretch, bond length growth	Extremely Significant bending, bond length shortening
	Fe-N Stretching vibration	/	Extremely significant Stretch, bond length growth	Extremely significant Stretch, bond length growth	/	Extremely significant Stretch, bond length growth	Extremely significant shrinkage, bond length shortening
	Fe(III)-C—N Bending vibration	/	Extremely significant Stretch, bond length growth	Extremely significant Stretch, bond length growth	/	Extremely significant Stretch, bond length growth	Extremely Significant bending, bond length shortening
	Fe-His Stretching	/	Extremely significant Stretch, bond length growth	Significant Stretch, bond length growth	/	Extremely significant Stretch, bond length growth	Extremely Significant bending, bond length shortening

Bond length means the linear distance between two atoms.

Discussion

Curing meat is popular among consumers and one of the most important techniques is wet curing (Gamage et al., 2017). Sodium nitrite plays an important role in the curing process and is a necessary additive when producing cured foods (Solano et al., 2013). During the meat curing process, sodium nitrite also serves as an inter-colour and anti-botulism agent (Lee et al., 2017), and available data indicate that sodium nitrite can form cherry-red NOMb with myoglobin in meat, leading to a bright red colour (Ahn et al., 2003). However, there have been no published studies on the dynamics of the binding site that binds sodium nitrite to myoglobin. Therefore, this study used previous research, FTIR, and microlaser confocal Raman spectroscopy to explore the impact of low sodium nitrite doses on the secondary structure and intermolecular forces associated with yak meat myoglobin during curing, which is another subject and novelty of this paper. These findings provide useful insights into sodium nitrite function and its mechanism during wet curing.

Sodium nitrite and myoglobin develop cherry-red NOMb during the meat curing phase, thereby giving the meat an appealing bright red colour (Gupta et al., 2018; Witting et al., 2001). This method includes three major reactions: 1) sodium nitrite oxidation of myoglobin to create

MetMb and nitric oxide; 2) the nitric oxide reaction with MetMb to create high nitrous iron myoglobin (nitrosylmetmyoglobin), which is not stable (McClure et al., 2011), and 3) reduction to light red NOMb in the presence of reducing substances in the meat. In this study, after curing with sodium nitrite, the Omb content significantly decreased, the MMb content increased and then levelled off, and the NOMb content steadily increased. The increase in MMb content was attributed to sodium nitrite oxidation, illumination, temperature and myoglobin autoxidation, and the plateauing was possibly due to the conversion of some myoglobin into NOMb and other reducing substances in meat. The NOMb content was positively associated with the curing phase, and the Omb, MMb and NOMb dynamics contributed to the stability of the redness values (a^*) for the cured yak beef (King et al., 2011).

Oxidation contributes to increased levels of dityrosine, a natural cross-linking covalent protein that facilitates protein aggregation (Mukherjee et al., 2019). The composition and size of the aggregates are correlated with changes in the turbidity of protein dispersions, which is another significant predictor of protein aggregation (Rifai et al., 2020). In this study, the addition of sodium nitrite facilitated the development of dityrosine myoglobin and increased turbidity, which in turn promoted myoglobin aggregation. Aggregation between proteins requires the involvement of free radicals (Mannino et al., 2020) and NO plays a

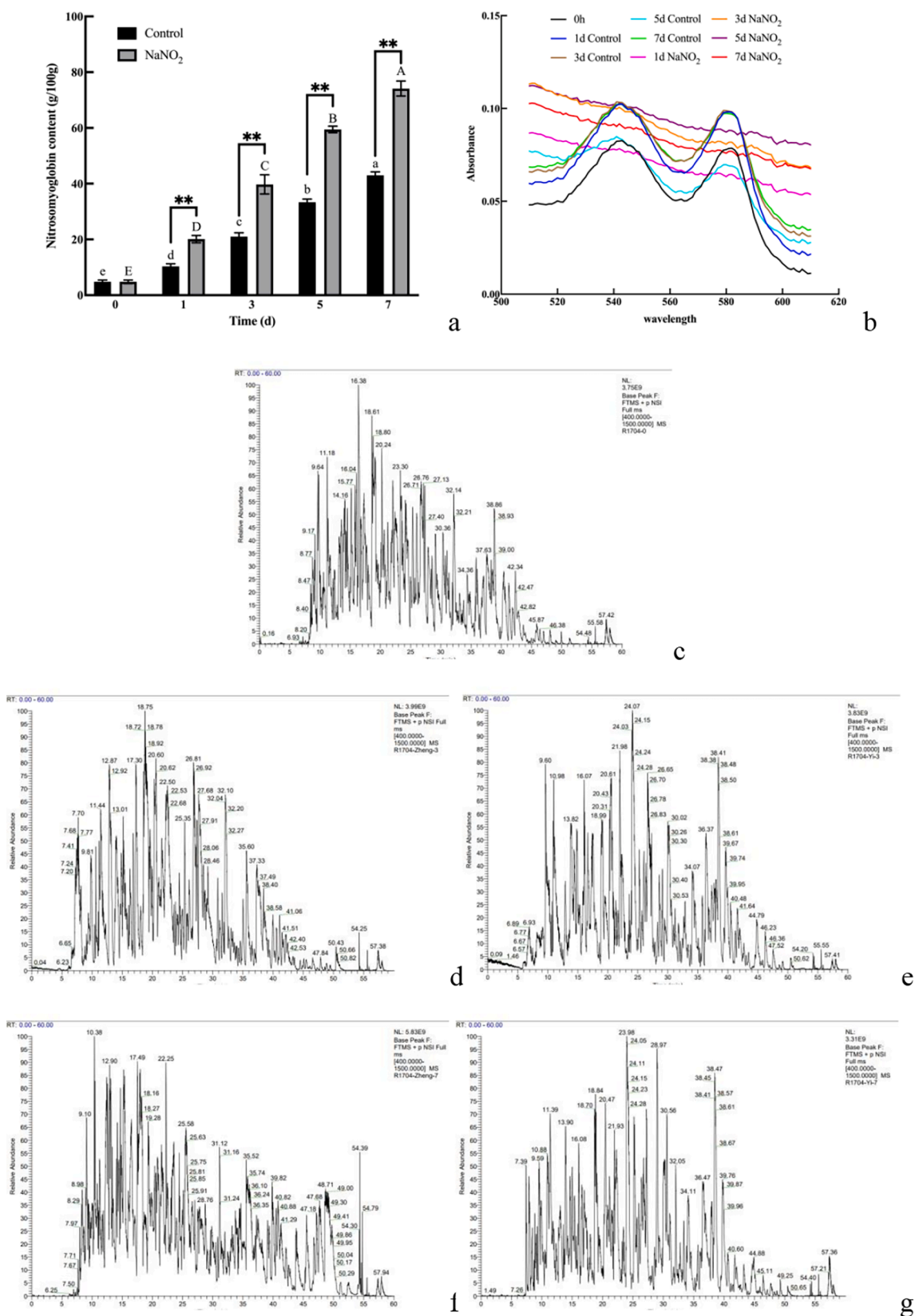


Fig. 3. Effect of sodium nitrite on nitrosomyoglobin content, visible spectrum of myoglobin and nitrosylation in yak meat. (a) nitrosomyoglobin content. (b) Visible spectrum of myoglobin at 510–610 nm. (c–g) LC-MS/MS primary mass spectra of nitrosylation. c: 0d, d: control 3d, e: NaNO₂ 3d, f: control 7d, g: NaNO₂: 7d. The small letters indicated the significant difference of the control group and the capital letters indicated the significant difference of the treatment group ($P < 0.05$). The * indicates the significant difference between groups, *: ($P < 0.05$); **: ($P < 0.01$).

Table 3
Identification results of nitrosylated peptides.

No.	Sequence	Length	Missed cleavages	Mass	Start and end position	Control			NaNO ₂			
						0d	3d	7d	0d	3d	7d	
1	ALEFRNDMAAQYK	14	1	1668.83	135	148	√	√	√	√	√	√
2	ALEFRNDMAAQYKVLGFHG	20	2	2279.15	135	154	√		√	√	#	#
3	ASEDLKK	7	1	789.42	58	64		#			√	#
4	ASEDLKKHGNTVLTALGGILK	21	2	2164.22	58	78			√			
5	FKHLKTEAEMK	11	2	1360.72	47	57	√	√	#	√		√
6	GHHEAEVK	8	0	905.44	81	88	√		√	√	√	
7	GHHEAEVKHLAESHANK	17	1	1892.92	81	97	√	√	√	√		
8	GHHEAEVKHLAESHANKHK	19	2	2158.08	81	99	√		√	√	√	
9	GLSDGEWQLVNLAWGK	16	0	1771.89	2	17	√	√	√	√	√	√
10	GLSDGEWQLVNLAWGKVEADVAGHGQEVLR	31	1	3345.71	2	32		√	√		#	#
11	HGNTVLTALGGILK	14	0	1392.81	65	78	√	√	√	√	√	√
12	HGNTVLTALGGILKK	15	1	1520.90	65	79	√	√	√	√	√	√
13	HLAESHANK	9	0	1005.50	89	97	√	#	√	√	√	#
14	HLAESHANKHK	11	1	1270.65	89	99	#	√		#	√	√
15	HLAESHANKHKIPVK	15	2	1707.95	89	103	√	√	√	√	√	√
16	HLKTEAEMK	9	1	1085.55	49	57	#	√	#	#		√
17	HLKTEAEMKASEDLK	15	2	1728.87	49	63		√			√	√
18	HPSDFGADAQAAMSK	15	0	1531.67	120	134	√	√	√	√	√	√
19	HPSDFGADAQAAMSKALELFR	21	1	2261.09	120	140	√	√	√	√	√	#
20	IPVKYLEFISDAIHVHLAK	20	1	2305.32	100	119	√		#	√		
21	KGHHEAEVK	9	1	1033.53	80	88	#	√	√	#		√
22	KGHHEAEVKHLAESHANK	18	2	2021.02	80	97		√	√			
23	KHGNTVLTALGGILK	15	1	1520.90	64	78	√	√	√	√	√	√
24	LFTGHPETLEK	11	0	1270.66	33	43	√	√	√	√	√	√
25	LFTGHPETLEKFDK	14	1	1660.85	33	46	√	√	√	√	√	√
26	LFTGHPETLEKFDKFK	16	2	1936.01	33	48	√	√	√	√	√	√
27	NDMAAQYK	8	0	939.41	141	148	√	√	√	√	√	√
28	NDMAAQYKVLGFHG	14	1	1549.73	141	154	√	√	√	√	√	√
29	TEAEMKASEDLK	12	1	1350.63	52	63	#	√	√	#		√
30	TEAEMKASEDLKK	13	2	1478.73	52	64	√	√	√	√	√	√
31	VEADVAGHGQEVLR	15	0	1591.83	18	32	√	√	√	√	√	√
32	VEADVAGHGQEVLRIFTGHPETLEK	26	1	2844.48	18	43		√	#		√	√
33	YLEFISDAIHVHLAK	16	0	1868.02	104	119	√	√	√	√	√	√
34	YLEFISDAIHVHLAKHPSDFGADAQAAMSK	31	1	3381.68	104	134	√	√	√	√		√

注: √: By MS/MS; #: By matching.

key role in the aggregation of myoglobin. Elevated levels of dityrosine indicate that the myoglobin has become oxidized, which corresponds to the elevated MMB levels. It has been suggested that nitrosylation of proteins prevents the formation of dityrosine, which in turn prevents protein cross-linking (Traore et al., 2012); however, the dityrosine content did not decrease in this study, possibly due to the oxidation of sodium nitrite.

The secondary protein structure is the local spatial structure of a peptide chain and is the bridge between primary and tertiary structures. There are four major types: α -helix, β -sheet, β -turns, and random coil. The stability of the structure is essential if the protein is to function correctly (Srou et al., 2017). In this study, the addition of sodium nitrite during the curing process resulted in loose and tight dynamic shifts in the myoglobin secondary structure, which improved the preservation of colour consistency and slowed colour degradation during the curing process. This result was consistent with the Raman spectroscopy findings. The myoglobin Raman spectrum reacts to the haem ring, the size of the haem core, the spin state of the Fe ions, and the distance between the Fe ions and the haem ring surface. The high-frequency area (1200–1700 cm^{-1}) describes the vibrational pattern of the haem skeleton and is a band that is sensitive to changes in haem composition. Minor distortions in the haem planar and axial Fe coordination bonds were expressed in the low-frequency range (200–700 cm^{-1}). Microscopic laser Raman spectroscopy analysis showed that sodium nitrite curing caused the myoglobin amide I (1340–1390 cm^{-1}), α -carbon and the nitrogen atoms to expand and then compress, which led to an increase in the stretch frequency. In amide III (1535–1575 cm^{-1}), the size of the middle part of the haem ring skeleton dynamically increased and then decreased. Therefore, the addition of low doses of sodium nitrite during the curing phase also helps preserve the complex shifts in myoglobin composition

and hence meat colour stability.

In this study, a total of 34 nitrosylated peptides were found, 15 of which were stable nitrosylated peptides that could be endogenous myoglobin nitrosylated peptides. Nineteen unstable nitrosylated peptides were detected and exogenous addition of sodium nitrite may be responsible for the interconversion of these nitrosylated peptides. As seen in Table 3, the interconversions among these unique, but dysfunctional nitrosylated peptides, may be the key factor leading to the bright red colour of the beef.

The bright red colour of meat is one of the most critical influences in the rise in the willingness of consumers to buy meat. Meat colour stabilization is a complex biochemical process, and meat scientists still deserve to research the role of sodium nitrite and the fundamental mechanisms at play.

Conclusion

In this study, the low-dose sodium nitrite treatment improved the redness of yak meat during wet curing and, after 3 days of curing, gave it a stable, bright red colour for four potential reasons: 1) the transformation of Omb and MMB into NOMB, which was the key cause for the bright red colour of yak meat; 2) the low sodium nitrite did promoted dynamic transformation of the myoglobin secondary structure and maintained its relative stability; 3) the low sodium nitrite did raised the interatomic vibration frequency of the central part of myoglobin haem and retained the dynamic haem balance and 4) the interconversions among dysfunctional nitrosylated peptides and sites were facilitated by the low sodium nitrite did treatment, which may be correlated with the bright red colour of yak meat.

CRediT authorship contribution statement

Guoyuan Ma: Investigation, Data curation, Formal analysis, Writing – original draft. **Zhuo Wang:** . **Qunli Yu:** . **Ling Han:** Project administration. **Cheng Chen:** . **Zhaobin Guo:** .

Declaration of Competing Interest

The authors declare that they have no known competing financial interests or personal relationships that could have appeared to influence the work reported in this paper.

Acknowledgments

This work was financially supported by the Scientific Research Start-up Funds of Gansu Agricultural University (GAU-KYQD-2021-19), the National Natural Science Foundation of China (No. 31771905, 31860426), Gansu Province Higher Education Industry Support Program (2020C-18), the Education Department of Gansu Province: Young Doctor Fund Project (Grant Nos: 2021QB-036) and the program for China Agriculture Research System (No. CARS-37).

References

- Ahn, H. J., Jo, C., Lee, J. W., et al. (2003). Irradiation and modified atmosphere packaging effects on residual nitrite, ascorbic acid, nitrosomyoglobin, and color in sausage. *Journal of Agricultural and Food Chemistry*, 51(5), 1249–1253.
- Bozkurt, H., & Erkmén, O. (2004). Effect of nitrate/nitrite on the quality of sausage (sucuk) during ripening and storage. *Journal of the Science of Food & Agriculture*, 84(3), 279–286.
- Chen, C., Han, L., Yu, Q. L., & Li, R. R. (2015). Color stability and antioxidant capacity of yak meat as affected by feeding with pasture or grain. *Canadian Journal of Animal Science*, 95(2), 189–195.
- China, S. A. C. (2018). *Operating procedure of livestock and poultry slaughtering—Cattle (GB/T 19477–2018)*. Beijing: Standards Press of China.
- Claus, J., & Du, C. (2011). Nitrite-embedded packaging film effects on beef color as influenced by meat age and muscle type. *Meat Science*, 96(1), 457–458.
- Das, R. S., & Agrawal, Y. K. (2011). Raman spectroscopy: Recent advancements, techniques and applications. *Vibrational Spectroscopy*, 57(2), 163–176.
- Denisa, H., Florina, S., Cristina, B., et al. (2018). The reaction of oxy hemoglobin with nitrite: mechanism, antioxidant-modulated effect, and implications for blood substitute evaluation. *Molecules*, 23(2), 350.
- Eberhardt, K., Stiebing, C., Matthäus, C., et al. (2015). Advantages and limitations of Raman spectroscopy for molecular diagnostics: An update. *Expert Review of Molecular Diagnostics*, 15(6), 773–787.
- Farhane, Z., Bonnier, F., Maher, M. A., Bryant, J., Casey, A., & Byrne, H. J. (2016). Differentiating responses of lung cancer cell lines to doxorubicin exposure: In vitro Raman micro spectroscopy, oxidative stress and bcl-2 protein expression. *Journal of Biophotonics*, 10(1), 151–165.
- Feng, X. C., Li, C. Y., Jia, X., et al. (2016). Influence of sodium nitrite on protein oxidation and nitrosation of sausages subjected to processing and storage. *Meat Science*, 116, 260–267.
- Gamage, H. G. C. L., Mutucumarana, R. K., & Andrew, M. S. (2017). Effect of marination method and holding time on physicochemical and sensory characteristics of broiler meat. *Journal of Agricultural Sciences*, 12(3), 172–184.
- Gupta, J., Bower, C. G., Gary, S., et al. (2018). Effect of differing ingredients and packaging technologies on the color of high-pressure processed ground beef. *Journal of Food Quality*, 1–5.
- Haile, D. M., Smet, S. D., Claeys, E., et al. (2013). Effect of light, packaging condition and dark storage durations on colour and lipid oxidative stability of cooked ham. *Journal of Food Science & Technology*, 50(2), 239–247.
- Honikel, K. O. (2008). The use and control of nitrate and nitrite for the processing of meat products. *Meat Science*, 78(1–2), 68–76.
- Kaspchak, E., Goedert, A. C., Mafra, L. I., & Mafra, M. R. (2019). Effect of divalent cations on bovine serum albumin (BSA) and tannic acid interaction and its influence on turbidity and in vitro protein digestibility. *International Journal of Biological Macromolecules*, 136, 486–492.
- Kuang, H., Li, Z., Peng, C., et al. (2012). Metabonomics approaches and the potential application in foodsafety evaluation. *Critical reviews in food science and nutrition*, 52(9), 761–774.
- Lee, J. H., Alford, L. D., Kannan, G., et al. (2017). Curing properties of sodium nitrite in restructured goat meat (chevon) jerky. *International Journal of Food Properties*, 20(3), 526–537.
- Li, K., Liu, J. Y., Bai, Y. H., et al. (2019). Effect of bamboo shoot dietary fiber on gel quality, thermal stability and secondary structure changes of pork salt-soluble protein. *CyTA-Journal of Food*, 17(1), 706–715.
- Luber, C. A., Cox, J., Lauterbach, H., et al. (2010). Quantitative Proteomics Reveals Subset-Specific Viral Recognition in Dendritic Cells. *Immunity*, 32(2), 279–289.
- Ma, G. Y., Chen, H., Zhang, Q., et al. (2019). Protective characterization of low dose sodium nitrite on yak meat myoglobin in a hydroxy radical oxidation environment: Fourier Transform Infrared spectroscopy and laser Micro-Raman spectroscopy. *LWT - Food Science and Technology*, 116, Article 108556.
- Mannino, M. H., Patel, R. S., Eccardt, A. M., et al. (2020). Reversible Oxidative Modifications in Myoglobin and Functional Implications. *Antioxidants*, 9(6), 549.
- McClure, B. N., Sebranek, J. G., Kim, Y. H., et al. (2011). The effects of lactate on nitrosylmyoglobin formation from nitrite and metmyoglobin in a cured meat system. *Food Chemistry*, 129(3), 1072–1079.
- Morzel, M., Gatellier, P., Sayd, T., et al. (2006). Chemical oxidation decreases proteolytic susceptibility of skeletal muscle myofibrillar proteins. *Meat Science*, 73, 536–543.
- Mukherjee, S., Fang, M., Kok, W. M., et al. (2019). Establishing Signature Fragments for Identification and Sequencing of Dityrosine Cross-Linked Peptides Using Ultraviolet Photodissociation Mass Spectrometry. *Analytical Chemistry*, 91(19), 12129–12133.
- King, D. A., Shackelford, S. D., & Wheeler, T. L. (2011). Relative contributions of animal and muscle effects to variation in beef lean color stability. *Journal of Animal Science*, 89(5), 1434–1451.
- Ramanathan, R., Suman, S. P., & Faustman, C. (2020). Biomolecular Interactions Governing Fresh Meat Color in Post-mortem Skeletal Muscle: A Review. *Journal of Agricultural and Food Chemistry*, 68(46), 12779–12787.
- Rifai, A., Asy'Ari, M., & Aminin, A. L. N. (2020). Anti-aggregation effect of Ascorbic Acid and Quercetin on aggregated Bovine Serum Albumin Induced by Dithiothreitol: Comparison of Turbidity and Soluble Protein Fraction Methods. *Jurnal Kimia Sains dan Aplikasinya*, 23(4), 129–134.
- Sassykova, L. R., Aubakirov, Y. A., Sendilvelan, S., Tashmukhambetova, Z. K., Zhakirova, N. K., Faizullaeva, M. F., et al. (2019). Studying the Mechanisms of Nitro Compounds Reduction (A-Review). *Oriental Journal of Chemistry*, 35(1), 22–38.
- Schwanhäusser, B., Busse, D., Li, N., et al. (2011). Global quantification of mammalian gene expression control. *Nature*, 473(7347), 337–342.
- Skibsted, L. H. (2011). Nitric oxide and quality and safety of muscle based foods. *Nitric Oxide*, 24(4), 176–183.
- Solano, M. R., Martinez, C. V., Cassada, D. A., et al. (2013). Effect of meat ingredients (sodium nitrite and erythorbate) and processing (vacuum storage and packaging atmosphere) on germination and outgrowth of Clostridium perfringens spores in ham during abusive cooling. *Food Microbiology*, 35(2), 108–115.
- Srouf, B., Bruechert, S., Andrade, S. L. A., et al. (2017). Secondary Structure Determination by Means of ATR-FTIR Spectroscopy. *Methods in Molecular Biology*, 1635, 195–203.
- Suman, S. P., & Joseph, P. (2013). Myoglobin Chemistry and Meat Color. *Annual Review of Food Science and Technology*, 4(1), 79–99.
- Tang, J., Faustman, C., & Hoagland, T. A. (2004). Krzywicki Revisited: Equations for Spectrophotometric Determination of Myoglobin Redox Forms in Aqueous Meat Extracts. *Journal of Food Science*, 69(9), C717–C720.
- Thiansilakul, Y., Benjakul, S., Park, S. Y., & Richards, M. P. (2012). Characteristics of myoglobin and haemoglobin-mediated lipid oxidation in washed mince from bighead carp (*Hypophthalmichthys nobilis*). *Food Chemistry*, 132(2), 892–900.
- Traore, S., Aubry, L., Gatellier, P., et al. (2012). Effect of heat treatment on protein oxidation in pig meat. *Meat Science*, 91(1), 14–21.
- Vossen, E., & Smet, S. D. (2015). Protein oxidation and protein nitration influenced by sodium nitrite in two different meat model systems. *Journal of Agricultural & Food Chemistry*, 63(9), 2550–2556.
- Wang, Z., Wu, X., Liu, L., et al. (2020). Rapid and sensitive detection of diclazuril in chicken samples using a gold nanoparticle-based lateral-flow strip. *Food chemistry*, 312, Article 126116.
- Witting, P. K., Douglas, D. J., & Mauk, A. G. (2001). Reaction of human myoglobin and nitric oxide. Heme iron or protein sulfhydryl (s) nitrosation dependence on the absence or presence of oxygen. *Journal of Biological Chemistry*, 276(6), 3991–3998.
- Wójcicki, K. M., & Dolatowski, Z. J. (2015). Effect of acid whey on nitrosylmyoglobin concentration in uncured fermented sausage. *Lwt - Food Science and Technology*, 64(2), 713–719.
- Zheng, X., Hu, Y., Anggreani, E., et al. (2017). Determination of total phenolic content and antioxidant capacity of blueberries using Fourier transformed infrared (FT-IR) spectroscopy and Raman spectroscopy. *Journal of Food Measurement & Characterization*, 11(4), 1909–1918.